Pulsed reaction spectrometry of DBD-mediated biogas reforming

K. Sakata[1], Y. Watanabe[1], Z. Sheng[1], S. Kameshima[1,2], H.-H. Kim[3], K. Okazaki[4], T. Nozaki[1]

[1] *Dept of Mechanical Engineering, Tokyo Institute of Technology, Tokyo, Japan*
[2] *The Japan Society for the Promotion of Science Research Fellow (DC1), Japan*
[3] *National Institute of Advanced Industrial Science and Technology, Japan*
[4] *Institution of Innovative Research, Tokyo Institute of Technology, Tokyo, Japan*

Abstract: Kinetic analysis of biogas reforming (CH_4, $CO_2 \rightarrow CO$, H_2) was performed over La-modified Ni/Al_2O_3 catalysts with dielectric barrier discharge (DBD). The reaction order for CH_4 and CO_2, as well as activation energy, were analysed within the scope of Langmuir-Hinshelwood surface reaction model. Reaction kinetics are further correlated with electrical properties of DBD at various conditions. Relationship between electrical properties and surface reaction, as well as DBD-induced synergism, were discussed comprehensively.

Keywords: Plasma catalysis, Packed-bed DBD, Pulsed reforming.

1. Introduction

Dry methane reforming (DMR, Eq. 1) is a promising reaction for low-calorific biogas upgrading:

$$CH_4 + CO_2 = 2H_2 + 2CO \quad \Delta H = 247\ \text{kJ/mol} \qquad \text{Eq. 1}$$

Nonthermal plasma-assisted DMR provides unique chemical reaction as well as energy input pathways. An appropriate combination of electrical energy provided by nonthermal plasma (ΔG) and the low-temperature thermal energy ($T\Delta S$) could satisfy the overall reaction enthalpy ($\Delta H = \Delta G + T\Delta S$) with higher energy conversion efficiency, which could initiate endothermic DMR at much lower temperature than thermal catalysis [1].

Nonthermal plasma-mediated catalytic gas conversion is recognized as *Plasma Catalysis* and packed-bed dielectric barrier discharge (DBD) reactor is used predominantly for this purpose [1]. Various positive effects have been reported so far such as increase in feed gas conversion, low-temperature catalyst activation and selectivity control [2]; however, the role of nonthermal plasma over the heterogeneous reaction is not always clear due to the complex discharge events and physicochemical interactions with catalysts. In this study, the kinetic analysis of biogas reforming was conducted in both thermal and plasma catalysis for the better insight into plasma-induced synergism.

2. Experimental system and procedure

Figure 1 shows schematic illustration of the packed-bed DBD reactor used in this study. The reactor includes quartz tube (I.D. 20 mm), 3 mm diameter high voltage electrode at the center, and the ground electrode outside of the quartz tube. Lanthanum modified Ni/Al_2O_3 catalyst pellets (Raschig ring type: φ3mm×3mm) were packed for 40 mm length (ca. 12 g; Ni 11 wt%; La 3wt%). The pore size of pellets was estimated to be smaller than 1 μm by the scanning electron microscope. A high voltage power source, generating quasi-sinusoidal waveform (12 kHz, 16 $kV_{p\text{-}p}$), was applied to the center electrode. Discharge power was measured by voltage-charge Lissajous analysis. Real time gas measurement was performed by a quadruple mass spectrometer (Prisma-100; Pfeiffer Vacuum GmbH). Catalyst bed was heated and controlled by an electric furnace: Meanwhile, the temperature distribution of the catalyst bed was measured by thermography (TH5104; NEC San-ei Instrument Ltd.) through the observation window. The emissivity of catalyst pellets was estimated to be 0.82 both in oxidation (NiO) and reduction (Ni) status. The temperature measured by thermography and the rotational temperature of CO, which represents plasma gas temperature, were matched within reasonable error [3].

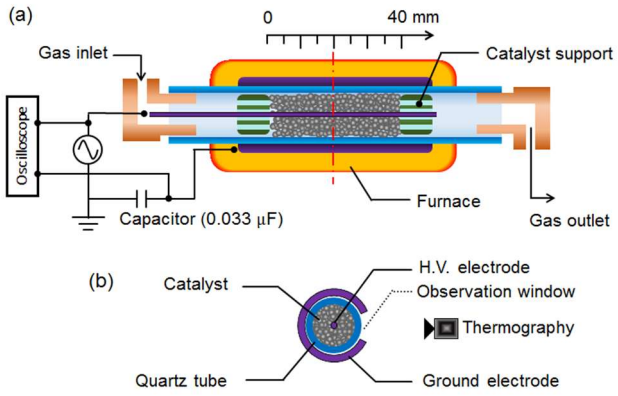

Fig. 1 Packed-bed DBD reactor: (a) overview, (b) cross-section view.

3. Experimental conditions and parameters

Experimental conditions are listed in Table 1. The Specific Energy Input (*SEI*) is calculated by Eq. 2 which represents discharge energy put into a unit volume of gas flow (J/cm^3) at standard temperature and pressure (101

kPa, 300 K). It is also interpreted as mean energy fed into a single molecule:

Table 1 Experimental conditions

	Plasma catalysis	Thermal catalysis
Power	90 W	–
SEI	1.25 eV/molecule	–
Total flow rate	1000 cm^3/min	
GHSV	5144 h^{-1}	
CH_4/CO_2	0.5, 0.64, 0.8, 1.0, 1.25, 1.5	
Pressure	5 kPa	
Catalyst Temp.	600 °C	

$$SEI = C \times \frac{P\ (W)}{Q_{total}\ (cm^3/min)}\ (\text{eV/molecule}) \qquad \text{Eq. 2}$$

P and Q_{total} represents respectively the discharge power and the total gas flow rate. C represents a conversion factor of the unit. Specific Energy Requirement (*SER*) for DMR is readily obtained from Eq. 1, showing *SER* = 247 kJ/mol = 2.56 eV/molecule: *SER* is correlated with *SEI* as follows:

$$SER = E + SEI \qquad \text{Eq. 3}$$

Eq. 3 expresses the conservation of energy for endothermic DMR and E presents thermal energy input per molecule supplied from the ambient low-temperature heat reservoir. It is hard to measure E experimentally because of complex heat transfer problem including heat generated by DBD. Conceptually, Eq. 3 implies the *SEI* should not exceed *SER* so that energy penalty of plasma catalysis is minimized. When *SEI* > *SER*, excess energy fed into the reactor is not utilized for DMR, but heating the reactor system. Gaseous hourly Space Velocity (*GHSV*) is calculated by the total gas flow rate divided by the reactor volume, showing the inverse of residence time. Kinetic analysis was performed by tuning *SEI* and *GHSV*.

4. Pulsed reaction spectrometry

Figure 2 shows overall pulsed reforming behavior and the corresponding catalyst bed temperature. One-cycle pulsed reaction consists of 10 min CH_4/CO_2 reforming followed by 10 min CO_2-DBD treatment. The CH_4/CO_2 ratio was incremented every cycle by the programmed mass flow controllers. When CH_4 content is greater than stoichiometric ratio (CH_4/CO_2 > 1, see Eq. 1), coke formation becomes prominent; CO_2-DBD treatment was conducted for 20 min so that coke is fully oxidized by CO_2 (Eq. 4)

$$C + CO_2 = 2CO \quad \Delta H = 172\ \text{kJ/mol} \qquad \text{Eq. 4}$$

Total amount of coke formed during 10 min reforming was measured quantitatively by integrating the consumption of CO_2 as illustrated in Fig. 2 (a):

$$\overline{F_C}\ (mg/min) = \frac{1}{10\ min} \times M_C \frac{P}{RT} \int_0^t Q_{CO_2}\,\mathrm{dt} \qquad \text{Eq. 5}$$

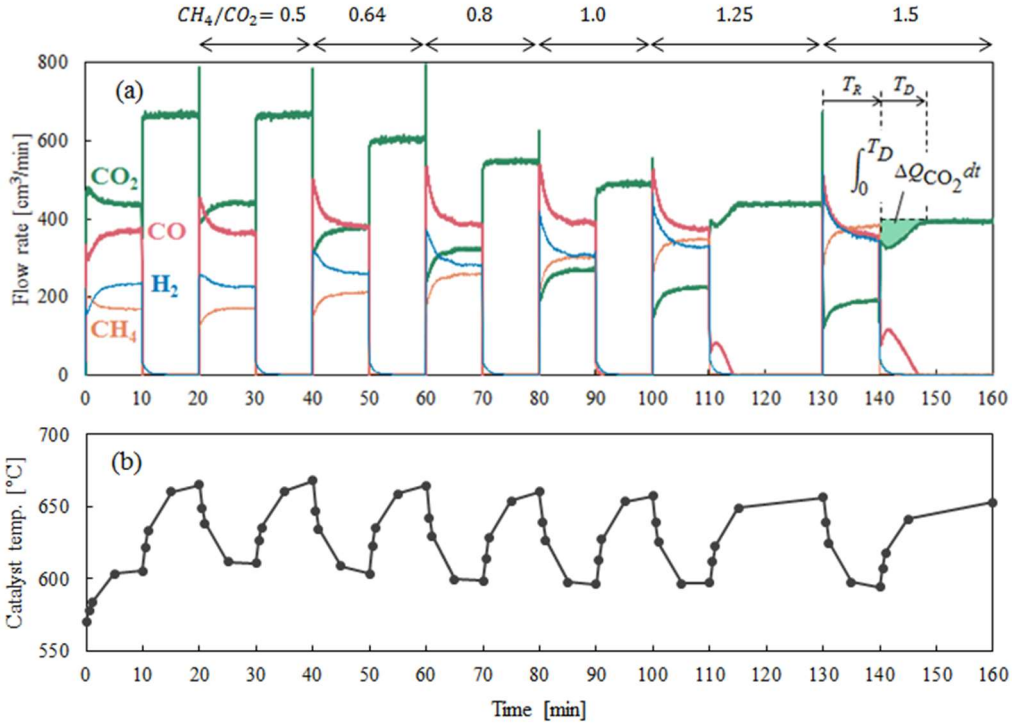

Fig. 2 (a) Time-dependent change of gas composition in plasma catalysis; (b) Corresponding catalyst temperature.

$\overline{F_C}$ represents mean coking rate. Temperature of the catalyst bed decreases during reforming period because of the endothermicity of DMR. After 10 min reforming, CH_4 flow is turned off and the temperature of the catalyst increases by the heat generated by CO_2-DBD. After steady state is confirmed by the gas profiles during reforming period, conversion of feed gas and product yield was calculated.

Figure 3 summarizes the conversion and the yield with respect to initial CH_4 fraction (x_{CH_4}) at a fixed catalyst temperature of 600 °C in both thermal and plasma catalysis: initial CO_2 fraction ($x_{CO_2} = 1 - x_{CH_4}$) is also provided as an auxiliary scale in Fig. 3 (a) and (b). CH_4 activation is initiated by dissociative chemisorption over the Ni catalyst, which is one of the slowest processes and thus known to be the key rate-determining step. It is quite encouraging that CH_4 conversion is increased clearly by DBD without increasing catalyst temperature. Likewise, CO_2 conversion as well as product yield were promoted by DBD. It is interesting to note that CO_2 conversion is independent of either CH_4 or CO_2 fraction between $0.3 < x_{CH_4} < 0.5$. This observation draws several important aspects. Generally, CO_2 adsorption is fast and bounded rather selectively near Ni and Al_2O_3 interface. Active cites for CO_2 are readily occupied, thus increase in CO_2 fraction does not either increase or decrease CO_2 conversion. In the case of plasma catalysis, adsorbed CO_2 is consumed to oxidize Ni to NiO [4,5] which eventually increases CO_2 conversion in plasma catalysis:

$$Ni + CO_2* = NiO + CO* \qquad \text{Eq. 6}$$

"*" denotes adsorbed species. Meantime, CO_2 conversion in plasma catalysis is still independent of either CH_4 or CO_2 fraction: adsorption of CO_2 is sufficiently fast and not influenced by DBD, but surface reaction enhancement by DBD (Eq. 6) would play the key role, providing abundant surface oxygen beyond thermal equilibrium [4]. In CH_4 rich condition (x_{CH_4} >0.5), coke formation becomes not negligible; correspondingly, CO_2 conversion and CO yield decreased because coke blocks the active cites for CO_2 adsorption.

In contrast, CH_4 conversion increase linearly with respect to CH_4 fraction, indicating CH_4 activation is in the adsorption-limited regime. However, it is hard to explain the CH_4 activation mechanism by DBD. Molecular beam study confirmed that vibrationally excited CH_4 has an ability to promote dissociative chemisorption over the nickel surface [6], and such reaction is highly possible in nonthermal plasma. However, DBD is characterized as weakly ionized discharge and electron number density, or current density, may not be sufficient to explain a macroscopic increase of CH_4 conversion (1.35~1.45 times increase). Moreover, deactivation of vibrationally excited CH_4, known as V-T relaxation, has a negative impact on synergism. One possible interpretation is the modification of catalyst by DBD, such as formation of nickel oxide [4] or lanthanum carbonate [7], would create new reaction pathways, promoting dissociative chemisorption of ground state CH_4.

5. Concluding remarks

In addition to pulsed reaction spectrometry, Arrhenius plot analysis is being conducted by the temperature-programmed analysis of DMR. The detailed reaction mechanism will be discussed based on apparent activation energy under the influence of DBD as well as DRIFTS FT-IR spectroscopy to identify catalyst modification by DBD. Nonthermal plasma-induced synergism and its mechanism is discussed comprehensively.

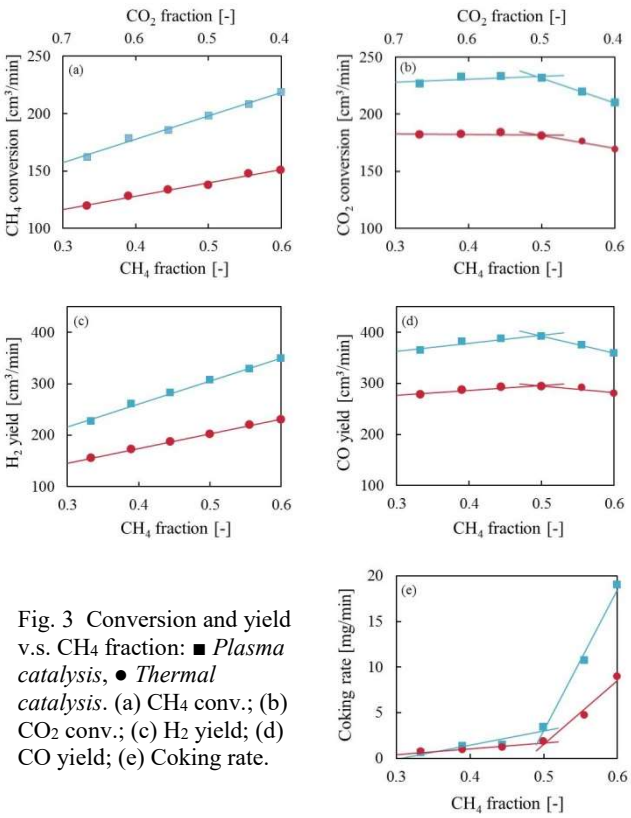

Fig. 3 Conversion and yield v.s. CH_4 fraction: ■ *Plasma catalysis*, ● *Thermal catalysis*. (a) CH_4 conv.; (b) CO_2 conv.; (c) H_2 yield; (d) CO yield; (e) Coking rate.

Acknowledgements

This work is supported partly by KAKENHI (JP16J09876). Z.R. acknowledges financial support from the program of China Scholarships Council (No.201707040056). S.K. is supported by the JSPS Research Fellowship for Young Scientists (DC1).

References

[1] Z Sheng et al, *Plasma Chemistry and Gas Conversion*, IntechOpen, pp.1-21, 2018.
[2] W-C Chung et al, *Catalysis Reviews*, Taylor & Francis, pp.1-62, 2018
[3] Y Du et al, *Plasma Chem. Plasma Proc.*, **37** (2017) 29-41.
[4] Z Sheng et al, *J. Phys. D: Appl. Phys.*, **51**, (2018) 445205(8pp).
[5] S Kameshima et al, *J. Phys. D: Appl. Phys.*, **51** (2018) 114006(8pp).
[6] A L Utz et al, *Catal. Today*, **244** (2015) 10-18.
[7] J Gao et al, *Fuel Cells: Technologies for Fuel Processing*, Elsevier, pp.191-221, 2011.